# Antimatter plasmas and antihydrogen*

R. G. Greaves and C. M. Surko[†,a)]
*Department of Physics, University of California, San Diego, California 92093-0319*

(Received 15 November 1996; accepted 15 January 1997)

Recent successes in confining antimatter in the form of positron and antiproton plasmas have created new scientific and technological opportunities. Plasma techniques have been the cornerstone of experimental work in this area, and this is likely to be true for the foreseeable future. Work by a number of groups on trapping antimatter plasmas is summarized, and an overview of the promises and challenges in this field is presented. Topics relating to positron plasmas include the use of positrons to study the unique properties of electron–positron plasmas, the interaction between positrons and ordinary matter, and the laboratory modeling of positron-annihilation processes in interstellar media. The availability of cold, trapped antiprotons and positrons makes possible the production of neutral antimatter in the form of antihydrogen. This is expected to enable precise comparisons of the properties of matter and antimatter, including tests of fundamental symmetries and the measurement of the interaction of antimatter with gravity. © *1997 American Institute of Physics.* [S1070-664X(97)92405-8]

## I. INTRODUCTION

The existence of antimatter has been known since Anderson's discovery of the positron in 1932,[1] and the role of antiparticles in elementary particle physics is now understood in great detail. Nevertheless, recent advances in the ability to capture and cool positrons and antiprotons in electromagnetic traps open up an exciting range of new scientific and technological opportunities. Many of these opportunities involve accumulating and manipulating large numbers of antiparticles. At present, the only practical way to accomplish this is through the creation of non-neutral antimatter plasmas. In this article we review current efforts to develop and use plasma techniques to accumulate antimatter. We also present an overview of the potential applications of antihydrogen and antimatter plasmas, including such topics as the study of fundamental aspects of electron–positron plasmas and the formation and study of cold antihydrogen.

The most easily produced and isolated antiparticles are the positron and antiproton. Positrons are now routinely used in a number of important applications, including positron emission tomography,[2] surface analysis, and atomic physics.[3,4] These topics, which have been discussed in detail in the reviews cited, do not normally require accumulations of positrons. Consequently, they fall outside of the scope of this article, and we will not discuss them further but concentrate instead on applications which hinge on the use of large numbers of cold, trapped antiparticles. We will also restrict discussion to the types of cold, non-relativistic antimatter plasmas that can now be created in the laboratory.

The history of confining and cooling antimatter in traps is extensive. The confinement of high energy positrons in a magnetic mirror was studied by Gibson *et al.* in the early 1960's.[5] The ability to confine small numbers of cold particles in Penning traps was developed by Dehmelt and coworkers at the University of Washington.[6] In 1978 Dehmelt proposed a technique for accumulating small numbers of positrons directly from a radioactive source, utilizing the magnetron drift of the particles.[7] This technique was experimentally demonstrated by Schwinberg *et al.*[8] They showed that single positrons can be confined for months, and they used the trapped particles for such experiments as the high precision measurement of the $g$-factor of the positron.[9]

The effort to accumulate larger quantities of antimatter was aided by the work of Malmberg and collaborators, who modified the Penning trap geometry to study cylindrical clouds of electrons sufficiently cold and dense to form plasmas.[10] They demonstrated that these pure electron plasmas have remarkably good confinement,[11,12] and this result has proven to be central to the creation of laboratory antimatter plasmas.

The excellent confinement properties of Penning traps make them a natural choice for the accumulation of antiparticles. For example, in order to accumulate positrons efficiently, we modified this type of trap to capture positrons from a radioactive source.[13,14] We are now able to accumulate more than $10^8$ positrons in a few minutes from a relatively compact and convenient radioactive source.[15] The resulting positron plasmas have a lifetime of about one hour. Similarly, antiprotons from the Low Energy Antiproton Ring (LEAR) at the European Laboratory for Particle Physics, CERN, have been trapped in Penning traps.[16–19] Currently, $10^6$ antiprotons have been captured and cooled to cryogenic temperatures in this kind of trap.[19]

These developments have created the opportunity for a range of new experiments. Studies of trapped antiprotons provide the most accurate measurement of the proton/antiproton mass ratio.[20] The interaction of low-energy positrons with atoms and molecules can be studied with precision in the isolated environment provided by a positron trap.[21–25] This environment is also suitable for modeling annihilation $\gamma$-ray processes of relevance to astrophysical phenomena.[26–28] Sufficient numbers of positrons can now be

*Paper 9RV1, Bull. Am. Phys. Soc. **41**, 1588 (1996).
[†]Review speaker.
[a)]Electronic mail: csurko@ucsd.edu

 1070-664X/97/4(5)/1528/16/$10.00 

routinely accumulated and cooled to form single component plasmas.[13,29] We have conducted the first electron–positron plasma experiments by passing an electron beam through a trapped positron plasma.[30]

Antihydrogen has recently been created for the first time by passing a beam of antiprotons through a xenon gas jet.[31] However, the atoms were too energetic to be trapped. Using trapped positron and antiproton plasmas for the production of cold antihydrogen, the capture and detailed study of neutral antimatter becomes possible.[32] This has attracted wide interest because it offers the opportunity to test CPT (charge, parity, time reversal) invariance with great precision and to measure the gravitational attraction between matter and antimatter.

This paper is organized in the following way. We first review confinement of single component plasmas in electrostatic traps. We go on to discuss the creation of positron plasmas, the trapping and cooling of antiprotons, and the formation of antiproton plasmas. We then review scenarios for the creation and trapping of cold antihydrogen atoms. Finally, we discuss current and anticipated uses of positron plasmas, cold antiprotons, and cold antihydrogen atoms.

## II. SINGLE COMPONENT PLASMAS

Penning traps with hyperboloidal electrodes were first used in the early sixties for the long-term confinement of small numbers of particles for precision measurements.[6] In 1975 Malmberg and deGrassie introduced the open-endcap cylindrical Penning trap for the study of plasma wave and transport phenomena in single component plasmas.[10] Although plasma studies had been conducted previously in this geometry (see, e.g., Ref. 33), it was Malmberg and coworkers who demonstrated the remarkably good confinement properties of electron plasmas in what are now called Penning–Malmberg traps. A wide variety of topics in plasma physics and fluid dynamics have been investigated using electron plasmas in Penning–Malmberg traps.[34–43] Penning traps of various geometries have also been used for the confinement of ions,[44] positrons,[13] and, most recently, antiprotons.[17,19]

A more recent variation of the Penning–Malmberg geometry is the ''orthogonalization'' of the well (i.e., the creation of an approximately harmonic potential over some volume in the center of the trap) by the use of compensation electrodes.[45] For small numbers of particles in Penning traps, such a harmonic potential possesses a characteristic bounce frequency, which is independent of amplitude. For large numbers of particles the system enters the plasma regime, i.e., the space charge of the plasma becomes appreciable and the Debye length, $\lambda_D$, becomes small compared with the size of the cloud. In this case, particles no longer experience a harmonic potential; the bounce frequency then depends on the plasma temperature and so the harmonic potential become less useful.

### A. Confinement limits

There are several constraints on the total number of particles, $N_t$, that can be accumulated in Penning traps. A space charge limit is imposed by the fact that the plasma tends to shield out the trapping potential. For a long cylindrical plasma of length $L$ and radius $R_p$, the space charge potential, $\phi_0$, at the center of the plasma is given by[46]

$$|\phi_0| = 1.4\times 10^{-7}\frac{N_t}{L}\left(1+2\log_e\frac{R_w}{R_p}\right) \quad \text{(V)}, \tag{1}$$

where $R_w$ is the wall radius of the trap. For example if $L=10$ cm and $R_w/R_p=2$, a confining potential of 1 kV would imply $N_t=3\times 10^{10}$ particles. For the short spheroidal plasmas confined in hyperboloidal wells, a scaling similar to the first term in Eq. (1) applies with the plasma radius setting the scale instead of $L$. In practice, long-term confinement of $10^{10}$ electrons in kilovolt wells is routinely achieved, and traps that can sustain confinement potentials of tens of kilovolts have been constructed.[18,47]

For particles in a quadrupole Penning trap, another limit is imposed by the radial electric field. For a given value of magnetic field, $B$, charge to mass ratio, $q/m$, and characteristic axial dimension of the trap, $z_0$, the confining potential must be kept below a critical value given by[48,49]

$$V_c = \frac{B^2 z_0^2 q}{4mc^2}, \tag{2}$$

where $c$ is the speed of light. This effect is reduced in long cylindrical plasmas where the radial electric field due to the confining electrodes is small except near the ends of the plasma.

A third confinement limit is imposed by a maximum achievable density $n_{\mathrm{B}}$, first described by Brillouin,[50] below which the repulsive and centrifugal forces on the rotating plasma can be balanced by the Lorenz force of the confining magnetic field:

$$n_{\mathrm{B}} = \frac{B^2}{8\pi mc^2}. \tag{3}$$

For positrons in a 1 T field, $n_{\mathrm{B}}\simeq 5\times 10^{12}\ \mathrm{cm}^{-3}$, while for antiprotons this value is $2.5\times 10^{9}\ \mathrm{cm}^{-3}$.

For antiprotons, the Brillouin limit is the practical limitation on the number of particles that can be accumulated. Densities of $0.1$–$0.2n_{\mathrm{B}}$ can be routinely attained, so for $B\sim 5$ T, up to $10^{10}$ antiprotons could conceivably be stored in a trap with typical axial and radial dimensions of a few centimeters. For positrons, the practical confinement limit will most likely be set by space charge. In this case the number of particles that could be accumulated would be determined by the maximum voltage that the trap can sustain.

### B. Plasma confinement

In a series of experiments, Malmberg and co-workers established that single component plasmas have remarkably good confinement properties.[10,11,34] The plasma confinement time, $\tau$, has been found to obey the scaling $\tau\propto(B/L)^2$, where $B$ is the magnetic field strength and $L$ is the length of the plasma.[38,35] The confinement time also depends on other plasma parameters, but no clear scalings have been identified. The good confinement can be understood in terms of the confinement theorem of O'Neil,[51] which analyzes the confinement of single component plasmas in terms of the ca-

nonical angular momentum. Under the assumption of azimuthal symmetry and no net torque on the plasma, O'Neil showed that the canonical angular momentum (which is proportional to the mean squared radius of the plasma) is strictly conserved. Thus the plasma is permanently confined. While this ideal result has not been achieved in practice, very long confinement times (i.e., hours or days) have been obtained by careful experimental design.[35] Any effect that exerts a net torque on the plasma leads to radial transport. These effects include viscous drag by residual gas atoms[34] and departures from azimuthal symmetry in the magnetic or electric field.[43,41] In many of the experiments conducted to date, the actual physical processes underlying transport of particles across the magnetic field are not understood.

Confinement of plasmas in hyperboloidal traps has not yet been studied in a systematic manner, but plasmas are known to diffuse out of such traps on timescales that are not very different from cylindrical traps of similar length (e.g., see Ref. 52).

### C. Plasma equilibria

It is now established that single component plasmas can be created in the laboratory in states that are close to thermodynamic equilibrium. In particular, such plasmas have a uniform temperature, equipartitioned thermal energy, and are free from rotational shear.[53] For long cylindrical plasmas in the low temperature limit (i.e., one in which the Debye length, $\lambda_D$, is much less than the size of the cloud), such an equilibrium implies a uniform density out to some surface of revolution, beyond which the density falls off in a way that can be described by a universal density function.[54] In hyperbolic traps, the equilibrium plasmas are spheroidal.[55]

A plasma that is in a non-equilibrium state will relax to the thermal equilibrium on characteristic timescales that depend on the plasma parameters. Equipartitioning of energy occurs on a timescale that is now well understood. The collision frequency scales as $T^{-3/2}$ in the high temperature, weakly magnetized regime [$r_c/b \gg 1$, where $r_c$ is the Larmor radius and $b = e^2/(k_B T)$ is the classical distance of closest approach, with $k_B$ being the Boltzmann constant]. This rate peaks for $r_c/b \sim 1$, and declines again for $r_c/b < 1$. These equilibration processes have been studied in detail, and there is now good agreement between theory and experiment.[36,37,56,57]

The internal transport of energy and particles across the magnetic field which leads to equilibrium radial profiles is less well understood, and can be influenced by a variety of processes. For an unstable plasma, the initial rapid evolution proceeds via the excitation of diocotron modes[58] or other two-dimensional $\mathbf{E}\times\mathbf{B}$ flow processes.[59] On longer timescales, collision transport to thermal equilibrium has been studied theoretically[60,61] and experimentally[39] and the transport rate is faster than would be expected on the basis of the ''classical'' values of the transport coefficients.[62,63] A recent experiment measuring the transport of spin tagged ions using laser fluorescence has observed transport rates that are about one order of magnitude larger than classical theory.[64]

### D. Plasma heating and cooling

Another plasma physics issue of importance for antimatter plasmas is plasma cooling. In Penning traps, plasmas can cool by cyclotron radiation,[36,37,65] by sympathetic cooling with other species in the trap (e.g., cooling of positron plasmas by their interaction with laser-cooled ions[66]), by collisions with gas molecules,[29] or by coupling energy to refrigerated circuit elements.[67] In the case of positron plasmas, cooling on a buffer gas is possible because the cooling time is at least one order of magnitude shorter than the annihilation time for simple molecules such as nitrogen. For long-term storage, where the buffer gas must be eliminated, cyclotron cooling is attractive. The cooling time for positrons is approximately $\tau \sim 4/B^2$(s) (where $B$ is in tesla),[36,37] and so using superconducting magnets with $B > 1$ T, cooling times of the order of one second are achievable. For antiproton plasmas, the cyclotron cooling time is quite slow because of the larger proton mass, and so in this case sympathetic cooling on an electron plasma confined in the same trap has been utilized[17,19] effectively.

Techniques have been developed to heat the plasma by applying rf noise to the confining electrodes or changing of the well depth. These techniques have been utilized to study relaxation to thermal equilibrium, plasma modes in electron plasmas, and the temperature dependence of positron annihilation rates in positron plasmas.[24]

### E. Plasma compression

If a torque is applied to a single component plasma in such a manner as to increase the angular momentum, the radial transport is inward, and the plasma will be compressed. A dramatic example of this effect was provided by recent experiments in trapped ion plasmas.[44] Off-axis laser beams were used to expand and compress ion plasmas, and densities close to the Brillouin limit were obtained.[68] Unfortunately, these laser techniques cannot be applied to elementary particles such as positrons and antiprotons. However, plasma compression is still possible using rotating electric fields coupled to the plasma through azimuthally segmented electrodes. Using this technique, plasma confinement times of several weeks have been obtained in an ion plasma, and recently increases in plasma density of a factor of 20 were obtained.[69] Such a capability will clearly be of great value for antimatter plasmas, because it can increase confinement times for long-term storage and provide higher densities, for example, for recombination experiments. It would also be of value for pulsed positron beams extracted from traps[70] because it would allow the restrictions of the Liouville theorem to be overcome: by compressing the plasma and allowing it to cool prior to beam extraction, the beam radius could be reduced and the phase space density thereby increased.

For small numbers of particles in harmonic potential wells, the technique of magnetron sideband cooling, which couples the azimuthal magnetron motion to the axial bounce motion, has been used to compress clouds of particles.[71] This technique is not applicable to plasmas, even when they are confined in quadratic wells, because the plasma space charge screens out the harmonic potential leading to an ill-defined

particle bounce frequency and a distortion of the magnetron frequency.

### F. Annihilation losses

Losses by annihilation are a key issue for antimatter plasmas. Annihilation rates depend on the density of the residual gas and the annihilation cross sections at the relevant particle energies. In the case of positrons, the annihilation cross section can be written as the dimensionless parameter $Z_{\mathrm{eff}}$ (which is not related to the spectroscopic parameter, $Z_{\mathrm{eff}}$, used in high density plasmas). This parameter relates the observed annihilation rate, $\Gamma$, to that of a gas of uncorrelated electrons, $\Gamma_0$,

$$\Gamma = \Gamma_0 Z_{\mathrm{eff}} = \pi r_0^2 c n_n Z_{\mathrm{eff}}, \tag{4}$$

where $r_0$ is the classical radius of the electron, and $n_n$ is the number density of the neutral gas molecules.[23] For simple gaseous elements such as $H_2$, $N_2$, and the noble gases, it is found that $Z_{\mathrm{eff}} \sim Z$, where $Z$ is the total number of electrons on the molecule. However, for larger molecules, especially hydrocarbons, $Z_{\mathrm{eff}}$ can exceed $Z$ by many orders of magnitude.[25,23] For this reason, vacuum systems completely free of hydrocarbon contaminants are required for positron storage. This precludes the use of diffusion or turbomolecular pumps. We have found ion pumps and cryogenic pumps to be suitable. We have created positron plasmas with a lifetime of about 40 s at a pressure of $\sim 5\times 10^{-7}$ of nitrogen, and the lifetime is expected to scale linearly with pressure as long as there are no high-$Z_{\mathrm{eff}}$ constituents in the residual gas. By extrapolating this number to $\sim 5\times 10^{-11}$ Torr (which is easily obtainable with commercial vacuum components), the lifetime is expected to be about 50 days.

For antiproton plasmas, the vacuum requirements are somewhat more stringent, because the annihilation cross section is larger than that of positrons. In particular, the capture cross section for low-energy antiprotons by atoms is $\gtrsim 100\pi a_0^2$, where $a_0$ is the Bohr radius.[72] Antiproton lifetimes of several months have been observed in systems at liquid helium temperatures,[16,17] and this has been used to infer pressures of $<10^{-16}$ Torr based on calculated antiproton annihilation cross sections.[72] In another experiment, antiproton lifetimes of about 1000 s were noted in a system with an estimated base pressure of $10^{-11}$ Torr.[19] Very recently, evidence has been presented that the antiproton annihilation rate at low temperatures in Penning traps may be lower than that predicted by the simple assumptions used to date.[19]

### G. Plasma diagnostics

Once an antiproton or positron plasma has been confined, the whole range of techniques developed to manipulate and diagnose electron plasmas can be applied. The trapped plasmas can be detected by lowering the voltage on the gate electrodes, allowing them to stream out along magnetic field lines onto a collector. The plasma temperature is measured directly by a ''magnetic beach'' energy analyzer,[73] or by measuring the number of particles collected as a function of the gate potential.[74] The total charge can be measured directly using a charge sensitive preamplifier. Radial profiles are measured by dumping the plasma onto a phosphor screen (or a microchannel plate followed by a phosphor screen) and imaging it using a CCD (charge coupled device) camera. For antimatter plasmas, measurements are often simplified by the fact that the annihilation radiation can also be detected—$\gamma$-rays in the case of positrons and annihilation pions for antiprotons. These events can be detected with a high degree of noise discrimination. By monitoring the annihilation products emitted from the trap, the annihilation rate can be measured without dumping the plasma.[19,24]

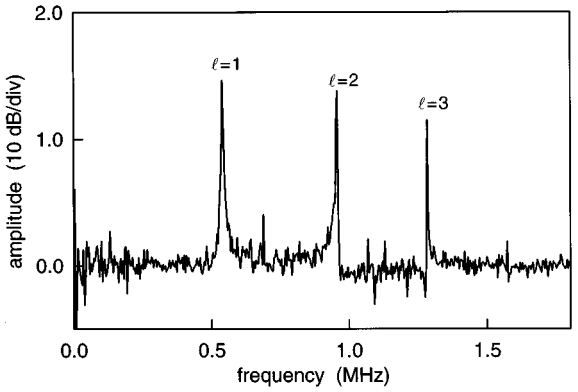


FIG. 1. Axial electrostatic modes in an antimatter plasma consisting of $\sim 7\times 10^7$ positrons. The $l=1$ mode is the center of mass mode and the $l=2$ and 3 modes are the first two axial compression modes.

The fact that these dense particle clouds in Penning traps are in a plasma state has advantages for non-destructive diagnostic purposes: the plasmas support a variety of collective plasma modes whose frequencies depend on global parameters such as the plasma shape, size, and temperature. An example of such modes is presented in Fig. 1. We have demonstrated the feasibility of using plasma modes to measure non-destructively the temperature, shape, and density of spheroidal electron or positron plasmas.[75,76] These techniques could also be applied to antiproton plasmas. For cold spheroidal plasmas, Dubin has derived an analytical dispersion relation for the electrostatic eigenmodes of the system,[77] and Bollinger *et al.* have derived the dispersion relation for certain asymptotic cases.[55] Experiments using cold pure electron plasmas have shown that these modes can be exploited as diagnostics of plasma density and shape,[52] while in warm plasmas, a correction to the cold fluid theory allows the plasma temperature to be obtained as well.[75,76] These modes have also been confirmed in numerical simulations.[78,79] The modes in question are axial electrostatic oscillations (analogous to Trivelpiece–Gould modes in plasma columns), but other branches of the dispersion relation have also been investigated in pure ion plasmas.[44,48,49,68]

## III. POSITRON PLASMA PRODUCTION

### A. Sources

At present, two types of positron sources are available, namely pair production (usually using electron linear accelerators) and radioactive sources. High energy $\gamma$-rays can produce positrons by pair production in specially designed

converters.[80,81] The required intense source of high energy $\gamma$-rays can be produced by bremsstrahlung using intense pulsed beams of electrons [e.g., from a LINAC (linear accelerator) with energies up to about 100 MeV] impinging on a high-$Z$ target. (The $\gamma$-rays can also be obtained in a nuclear reactor from neutron capture reactions such as $^{113}\mathrm{Cd}+n\rightarrow{}^{114}\mathrm{Cd}+\gamma$.[82]) Electron LINACs are copious sources of positrons, and the positron pulses that they produce are, at least in principle, relatively simple to trap by switching electrode voltages with appropriate timing.

Many radioisotopes decay by positron emission, and several of these are available commercially. In early experiments, relativistic positrons from radioactive neon gas were trapped directly in a magnetic mirror device.[5] Short-lived isotopes such as $^{64}$Cu can be used as positron sources, but they must be prepared on site in a nuclear reactor.[83] Currently, the most commonly used positron emitter is $^{22}$Na, which has a half-life $\tau_{1/2}\simeq 2.6$ yr and is available as a sealed source with activities up to 150 mCi. Other commercially available positron sources include $^{58}$Co and $^{68}$Ge. Short-lived isotopes such as those used for positron emission tomography (e.g., $^{11}$C, $^{14}$N, $^{15}$O, or $^{18}$F) can be produced on site, using proton or deuteron beams from small cyclotrons or other compact accelerators with energies of a few tens of MeV[2] and this technique as also being investigated for positron beam systems.[84,85]

### B. Positron moderators

Positrons from either a radioactive source or from a LINAC have a broad range of energies up to several hundred keV, and for efficient trapping the positrons must be slowed to energies of a few electron volts. Typically this is accomplished using a solid-state moderator.[86] Several types of moderators are available including metal single crystals, insulators such as MgO and SiC, and rare gas solids.

Single crystals of various metals have traditionally been used to obtain slow positrons. Tungsten,[87] nickel,[88] and copper[89] have been demonstrated as moderators, although tungsten is used most widely. These metals are used either in reflection geometries or as foils in transmission geometries, and they typically have moderation efficiencies of about $1-2\times10^{-4}$, defined as the ratio of the number of slow positrons emitted to the activity of the source. The energy spread of the emitted positrons can be as low as 30 meV for refrigerated moderators,[90] but values of a few tenths of an eV are more typical at 300 K.

An important recent advance in positron moderator technology is the discovery that rare gas solids can moderate positrons about an order of magnitude more efficiently than metal single crystals.[91] In a typical geometry, the positron source is recessed into a conical or parabolic cup mounted on a cold head.[92] A closed cycle refrigerator is used to cool the source and a layer of rare gas freezes onto the source. Neon has the highest moderation efficiency, although argon, krypton, and xenon perform reasonably well.[91,93] We have recently demonstrated the use of a two-stage refrigerator for the production of neon moderators,[94] which require temperatures of $<8$ K. This results in a considerable cost-saving over the three-stage units that were previously required to reach this temperature. Moderation efficiencies (as defined above) of about 0.006 are commonly obtained for krypton and neon. An alternative definition of moderation efficiency is the number of slow positrons emitted per incident fast positron. For neon moderators this is typically $\sim 2.5\%$.

### C. Trapping positrons

Positrons can be accumulated in traps if a suitable mechanism is used to extract energy while the positrons experience the trapping potential. A variety of techniques have been investigated. These include the magnetron drift technique, first proposed by Dehmelt *et al.*[7] and experimentally demonstrated by Schwinberg *et al.*,[8] collisions with buffer gas molecules[25,14] or with ions,[66] ramping the potential on the positron source,[95] or from the chaotic orbits of positrons from vane moderators.[96] If a pulsed source is available, positrons can be trapped by rapid switching of the confining potential. This technique has been implemented on several LINACs for a variety of purposes.[97–101] Two techniques have been experimentally demonstrated for the accumulation of large numbers of positrons from radioactive sources in Penning traps, namely, the magnetron drift technique[102] and the buffer gas method.[29]

With the magnetron drift technique, positrons are injected into a Penning trap off-axis through a small hole in one of the endcap electrodes from either a radioactive source[8] or from a moderated source.[102] Some positrons are reflected by the opposite endcap and can magnetron-drift away from the field line on which they entered, to become trapped. The trapped positrons are cooled by coupling their energy into a resonant circuit connected to the confining electrodes or by cyclotron emission. The efficiency of this scheme is very low ($\sim 10^{-5}$).

In the buffer gas method, moderated positrons from a radioactive source are trapped by inelastic scattering collisions with molecules of a buffer gas.[14,29] The source is $^{22}$Na, which emits positrons with energies up to 540 keV. The positrons slow down to a few electron volts in a solid neon moderator[91,94] and accumulate in the trap by electronic excitation of $N_2$ molecules.

Our trap, which is shown schematically in Fig. 2, is formed by a set of eight cylindrically symmetrical electrodes of varying lengths and radii. Nitrogen is introduced into the first stage, and differential pumping maintains a pressure gradient of about three orders of magnitude between the first and third stage, thus creating a low-pressure region where the positrons can be accumulated without rapid annihilation on the nitrogen gas molecules. The potential profile, shown in Fig. 2, is produced by applying appropriate voltages to the individual electrodes. Positrons accumulate in the lowest potential region (stage III) following a series of inelastic collisions, marked ''A,'' ''B,'' and ''C'' in Fig. 2. The high pressure in stage I permits good trapping efficiency by assuring a high probability of collision during the first pass. The electrode potentials are carefully tuned to maximize the probability of an inelastic collision while avoiding positronium atom formation, which is a loss mechanism. The highest efficiency has been obtained using electronic excitation of nitrogen at 8.8 eV.[14] Using nitrogen, the overall efficiency

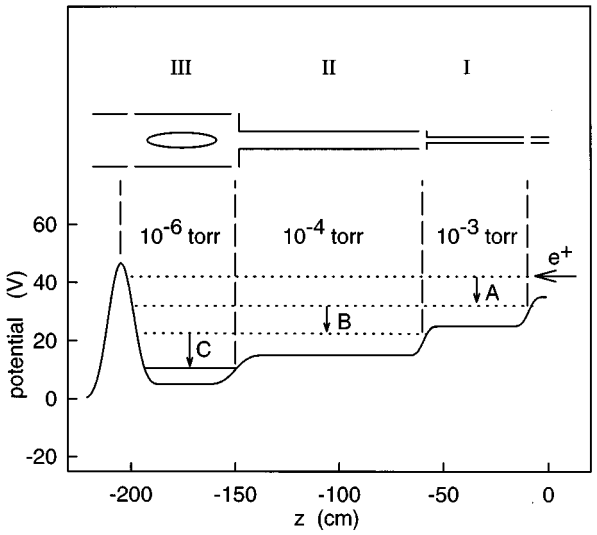


FIG. 2. Schematic diagram of a three-stage positron trap, showing the electrodes (above), which create three regions of successively lower pressure and potential (below). Nitrogen gas is admitted in the center of the stage I electrode. A magnetic field of 1 kG is aligned with the axis of the trap.

of the trap for capturing low-energy positrons is remarkably high—25% using a neon moderator and 40% using the lower efficiency tungsten moderators (which have a narrower energy spread). As shown in Fig. 3(a), we can now accumulate up to $10^8$ positrons in a few minutes.

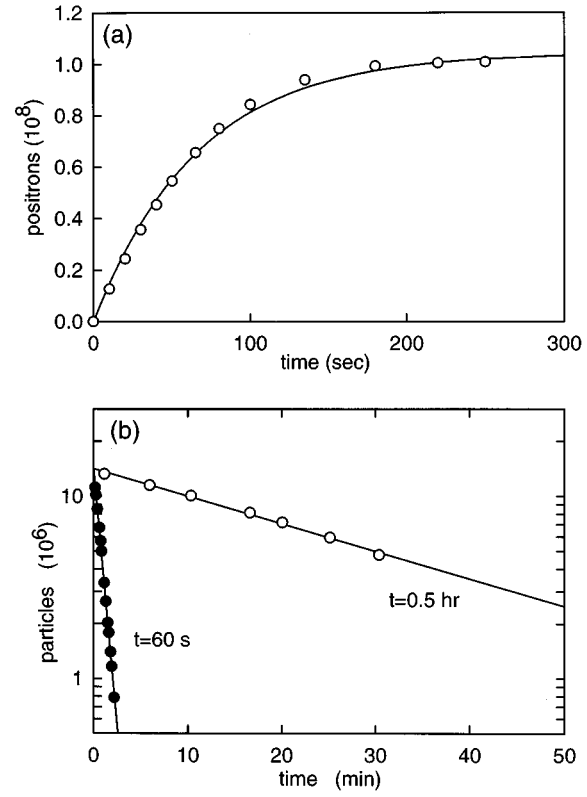


FIG. 3. (a) Filling of a trap with positrons from a 65 mCi $^{22}$Na source. (b) Storage of positrons after the source and buffer gas feed are switched off: (●) $p=5\times10^{-7}$ Torr and (○) $p=5\times10^{-10}$ Torr.

As shown in Fig. 3(b), the positron lifetime is about one minute at a nitrogen gas pressure of $5\times10^{-7}$ Torr. If the buffer gas feed is switched off after the positrons have been loaded into the trap, the pressure falls to the base pressure of the device ($5\times10^{-10}$ Torr) in about 30 s.[103] Under these conditions, the positron lifetime is about half an hour. The ability to stack plasmas (i.e., to add extra particles in batches to a stored plasma) is very important for the accumulation of large numbers of antiparticles. For positrons, we have demonstrated this ability by shuttling and stacking plasmas from the third stage to the fourth stage of our trap.[29]

## IV. ANTIPROTONS IN TRAPS

### A. Antiproton production

Antiprotons are produced in collisions of high-energy protons with a solid target. At present the most copious source of low-energy antiprotons is the Proton Synchrotron-Low Energy Antiproton Ring (PS-LEAR) complex at CERN.[104] Protons are accelerated to 28 GeV/c by the synchrotron and produce antiprotons by collision with a conversion target. Antiprotons at about 3.5 GeV/c are collected in the Antiproton Collector (AC) ring where up to $10^{12}$ $\bar{p}$ can be stored for weeks or months. Batches of $10^9$–$10^{10}$ $\bar{p}$ can be skimmed off and decelerated in the PS to 600 MeV/c, and then transferred to LEAR where they can be further decelerated to ~100 MeV/c. Antiprotons can then be extracted from LEAR in batches of up to a few times $10^9$ and passed into an energy degrader (for example, Al or Be foils) where a few percent of the $\bar{p}$ are decelerated to energies of $<50$ keV. At these energies the particles can be trapped in a conventional Penning trap by rapidly switching the confining potentials.[16,19]

### B. Trapping and cooling of antiprotons

Once antiprotons have been trapped, they can be cooled further by sympathetic cooling with electrons, which can be conveniently confined in the same trap. The electrons cool much more rapidly by cyclotron radiation than the antiprotons, and the antiprotons transfer their energy rapidly to the electrons by collisions. Using this technique, it is possible to obtain antiproton temperatures close to that of the trap (e.g., ~4 K). The number of antiprotons stored can be increased by stacking and cooling several batches of antiprotons. As shown in Fig. 4, up to $1\times10^6$ antiprotons have been captured in this way.[19,105]

LEAR was decommissioned in December 1996, but it is proposed to reconfigure the Antiproton Collector at CERN to form an antiproton decelerator (AD), which will enable the resumption of low-energy antiproton production in 1999. Two collaborations (PS200/ATHENA and PS196/ATRAP) plan to develop methods to produce and study antihydrogen using this facility.

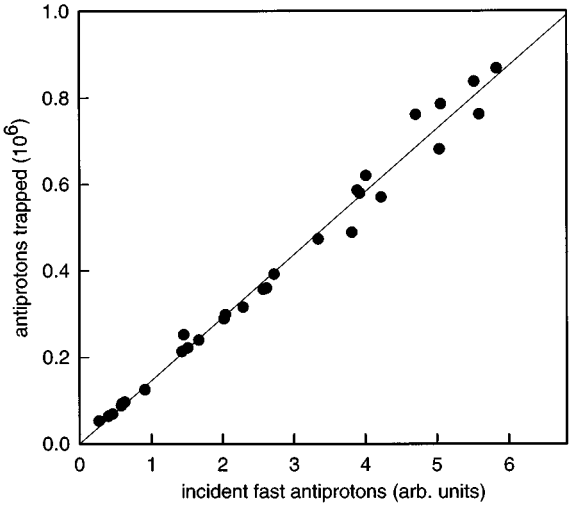


FIG. 4. Number of antiprotons captured in the PS200 Penning trap as a function of the number of antiprotons in the incoming pulse from LEAR (after Ref. 105).

## V. ANTIHYDROGEN PRODUCTION

### A. Recombination reactions

Several methods have been proposed for antihydrogen formation, and they can be summarized by the following reactions.

*Spontaneous radiative recombination.* Antiprotons and positrons can recombine by the spontaneous emission of a photon, but the recombination rates are relatively low,

$$\overline{p}+e^+\rightarrow\overline{\mathrm{H}}+h\nu. \tag{5}$$

*Laser-stimulated recombination.* In this process, emission of the photon is stimulated by pumping at a suitable laser frequency:

$$\overline{p}+e^++h\nu\rightarrow\overline{\mathrm{H}}+2h\nu. \tag{6}$$

The reaction rate can be enhanced by one or two orders of magnitude over the spontaneous recombination rate. This reaction has been experimentally demonstrated for protons and electrons in a merged beam geometry,[106] but it has not yet been attempted using trapped plasmas.

*Three-body recombination.* This reaction is mediated by a second positron, which carries off part of the binding energy, leading to significantly increased reaction rate,[107]

$$\overline{p}+e^++e^+\rightarrow\overline{\mathrm{H}}+e^+. \tag{7}$$

The reaction rate scales as $T^{-4.5}$, so that in principle very large enhancements are possible at low temperatures.[107] A major disadvantage is that the antihydrogen atoms are expected to be produced in highly excited, long-lived Rydberg states, which are susceptible to collisional and field ionization, a problem which is accentuated by the space charge of the plasma.

*Charge-exchange collisions with positronium atoms.* This reaction has a relatively large cross section ($\sim 10^{-15}\,\mathrm{cm}^2$) and favors low-$n$ states that are stable to re-ionization:[108]

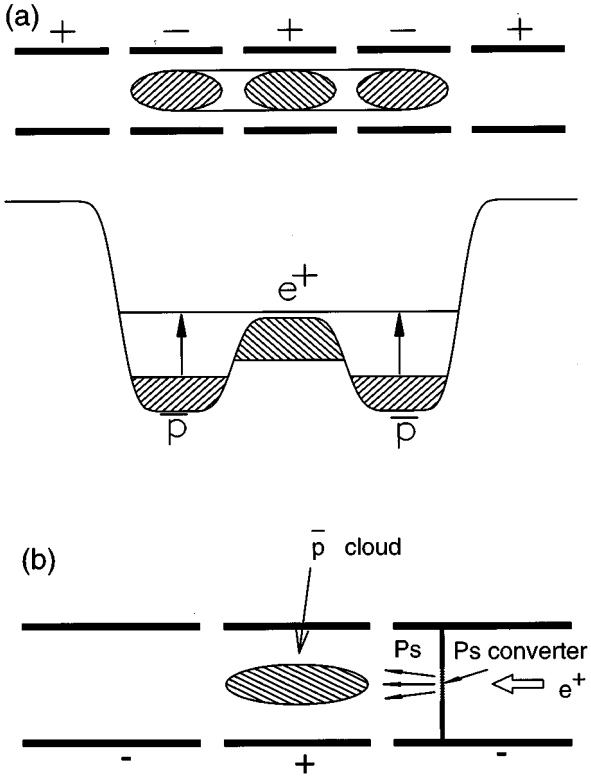


FIG. 5. Two of the proposed schemes for producing antihydrogen: (a) Nested traps employing three-body recombination [Eq. (7)] or laser-stimulated recombination [Eq. (6)]; (b) charge-exchange collisions with positronium atoms [Eq. (8)], produced when incoming pulses of positrons strike a positronium converter close to the antiproton cloud.

$$\overline{p}+\mathrm{Ps}\rightarrow\overline{\mathrm{H}}+e^-. \tag{8}$$

The reaction rate can be enhanced by using excited states of positronium, and the reaction rate scales as $n^4$,[109] where $n$ is the principle quantum number of the excited Ps atom. This reaction has already been demonstrated using protons and positronium atoms.[110] One disadvantage of this method is that, if ground state positronium is used, the resulting antihydrogen atoms are too hot to be trapped efficiently (i.e., kinetic energy $\sim$27 K). This can potentially be overcome using excited state positronium.[109]

### B. Experimental geometries

Figure 5 shows two of the possible geometries for producing antihydrogen. Figure 5(a) shows the nested trap geometry,[111,112] in which an outer trap confines the antiprotons while an inner trap confines the positrons. In this geometry, overlap of the plasmas might be difficult to achieve because the plasmas will tend to separate into their respective wells as illustrated in Fig. 5. Overlap could be facilitated by heating the antiprotons or injecting them with high energy into the trap. The antiprotons will cool on the positrons on a faster timescale than they equilibrate with the potential well, and so a relatively long-lived overlapping configuration might be obtained, although the stability properties of this system are not known. Such a system could be suitable for the three-body recombination reaction. This geometry has been tested experimentally using proton and electron

plasmas.[112] Proton cooling was observed but no recombination was reported, perhaps because of re-ionization of the Rydberg atoms.

A possible geometry for implementing the positronium atom scenario is illustrated in Fig. 5(b). An incoming pulse of positrons strikes a positronium converting surface close to the antiproton cloud. The resulting positronium atoms pass through the cloud producing antihydrogen atoms by charge exchange.[113]

Another possible geometry for implementing the three-body recombination reaction is the combined trap (or Penning–Paul trap), in which the antiprotons are confined in the usual way using the Penning geometry while the positrons are confined by rf fields.[114,115] One difficulty to be overcome for this scheme is minimizing rf heating so that sufficiently cold particles for recombination can be obtained.

### C. Trapping antihydrogen

Since it is electrically neutral, antihydrogen cannot be trapped in electrostatic or rf traps. However, neutral atoms with a permanent magnetic dipole moment, $\boldsymbol{\mu}$ (which in antihydrogen is dominated by the positron's dipole moment), can be confined in an inhomogeneous magnetic field, because atoms with $\boldsymbol{\mu}$ antiparallel to the field will be drawn to the minimum in the magnetic field.[116] With $B=1$ T, gradients can be produced that are large enough to trap antihydrogen atoms up to 0.67 K (0.055 meV). Various geometries are possible, ranging from the simple two-coil quadrupole to multi-coil Ioffe-traps. The latter type of trap has been employed recently to confine hydrogen for precision spectroscopy.[117] However, as described in Sec. II B, there is a potential problem in confining antihydrogen in close proximity to a Malmberg–Penning antiproton trap, since it will need to be coaxial with the antiproton trap, and such an azimuthally asymmetrical magnetic geometry is known to be unfavorable for single component plasma confinement.[51]

Once the antihydrogen has been trapped, it must be cooled further if very precise spectroscopic measurements are to be made. The evaporative cooling[116] method that is currently used in trapped hydrogen experiments is out of the question, because large numbers of antihydrogen atoms would be required. Instead, it appears that laser cooling must be employed.[118]

This field of research is in its infancy. Thus it is easy to miss key points that, while not presently appreciated, could become crucial to future developments. In the case of positron trapping, the unanticipated large annihilation rate for low-energy positrons interacting with large hydrocarbon molecules affected the development of positron traps in a central way. A similar turning point might arise if, for example, antihydrogen atoms were found to have a significant reflection coefficient from solid surfaces. The ability to rely on several bounces from solid walls before annihilation could simplify the trapping of antihydrogen atoms.

## VI. USES OF ANTIMATTER

### A. Uses of positrons

#### *1. Electron–positron plasmas*

The behavior of plasmas composed of electrons and positrons differs from conventional plasmas in fundamental ways. In contrast to electron–ion plasmas, both charge species have the same light mass. Electron–positron plasmas are believed to occur naturally in astrophysical environments such as pulsar magnetospheres[119] and active galactic nuclei.[120] These plasmas are currently the subject of intensive theoretical and numerical investigation, both in the relativistic and non-relativistic regime.[121–126]

The linear modes of electron–positron plasmas have been considered in detail, and in many respects they are similar to those in more conventional plasmas.[127–129] However, in a seminal paper, Tsytovich and Wharton showed that the non-linear processes are dramatically different.[130] In the important case of equal temperatures and equal densities for positrons and electrons, three-wave coupling vanishes identically. This implies, for example, that quasilinear relaxation of a beam–plasma instability is absent. Furthermore, because of the light masses of both particles, ordinary non-linear Landau damping (NLLD), which is dominated by the ions in conventional plasmas, is larger by the ion-to-electron mass ratio. Consequently, non-linear growth can overwhelm linear growth, and quasilinear relaxation is replaced by very strong non-linear Landau damping. In one step, energy can be coupled directly into the bulk of the particle distribution. Wharton and Tsytovich also pointed out that the properties of solitons can be expected to be distinctly different in electron–positron plasmas. Due to the fact that the sound mode is absent, solitons cannot decay by radiating sound as they do in ordinary plasmas, but slow down and stop (due to NLLD).

The developments discussed above, which now enable the creation of robust positron plasmas in the laboratory, will allow us to test these predictions in this qualitatively different plasma system. Recently we have performed the first electron–positron plasma experiment. While we are not yet able to confine electrons and positron plasmas in the same volume simultaneously, we have been able to study the effect of an electron beam passing through a positron plasma in the important case where the beam and plasma densities are equal. Figure 6 shows an example of the types of phenomena that can be studied in this system. Intense heating of the plasma is observed, arising from a type of two-stream instability.

An important goal of this research will be to study simultaneously confined electron–positron plasmas. As we discuss in Sec. V, configurations of ''nested'' Penning traps, such as that shown in Fig. 5(a), cannot be used to accomplish this. When both species are plasmas, they fall into separate wells and overlap only over one Debye length. If heated, the particles can be confined in the same volume, but then the Debye length is comparable to the spatial extent of the charge cloud, and the system is not in the plasma regime. We are currently considering the use of a Paul trap to achieve simultaneously confinement of electron and positron plas-

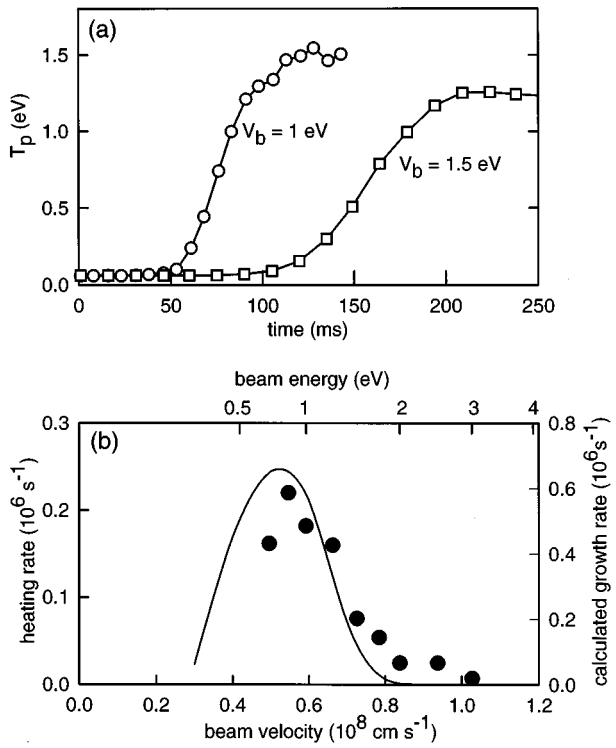


FIG. 6. (a) Positron heating caused by the interaction of an electron beam with a stored positron plasma for two values of electron beam energy. (b) (●) measured heating rates; solid line: theoretical predictions of the growth rate of the dominant unstable mode (Ref. 30).

mas. In this case, the ponderomotive force due to the rf electric field provides a potential well which is identical for both charge species. However, this confinement mechanism is expected to produce significant plasma heating, and consequently its success will require an efficient cooling mechanism.

Electron–positron plasmas also offer the opportunity to study important plasma confinement questions. Since both particles have the same small mass, they can be equally and strongly magnetized by magnetic fields currently available. This should permit studies of confinement in new and potentially interesting regimes not possible with other plasmas.[131,132]

Given the intrinsic interest and extensive theoretical literature in the area of relativistic electron–positron plasmas, it would be of great value to be able to study this regime experimentally. Unfortunately, the required positron densities appear to be very difficult to achieve. For example, creation of an electron–positron plasma with a temperature of 1 MeV and $\lambda_D = 1$ cm requires a plasma density of the order of $5\times10^{11}$ cm$^{-3}$. Thus a plasma ten Debye lengths in spatial extent in each direction would require trapping in excess of $10^{14}$ positrons. Since the current record is $10^8$ positrons, trapped at much lower energies where long-time confinement is easier, this does not appear likely in the near future. The most promising geometry is probably an intense, pulsed electron beam source and magnetic mirror trap, as described by Wharton and Tsytovich.[130]

While the relativistic plasma regime seems to be difficult to achieve in the laboratory, an experiment is currently underway to study energetic positrons, confined in a magnetic mirror with the aid of intense cyclotron heating.[133] In this case, the positrons come from a radioactive source and solid-state moderator. Of interest is the study of the unique radiation properties of electron–positron gases. Other experiments are underway to accumulate positron plasmas in Penning traps using LINAC sources.[97,98]

With regard to astrophysically relevant positron physics, the slowing down of positrons in partially ionized electron–ion plasmas raises a number of important issues related to understanding the mechanisms for positron annihilation in interstellar media. This has been considered in detail theoretically.[134–136] A number of these issues can now be addressed in modest-scale laboratory experiments with the techniques described above.[26,27]

### 2. Positron–molecule interactions

Another facet of low-energy antimatter research relates to atomic and molecular physics. While many aspects of the interaction of low-energy positrons with solids, liquids, and dense gases have been studied for decades, the ability to isolate two-body positron–atom and positron–molecule interactions has been aided greatly by the advent of efficient positron traps. One example is the study of positron–molecule and positron–atom interactions below the threshold for positronium formation.[25,21–24,137] This is an important class of problems in atomic and molecular physics in that these problems address the physics of the interaction of a light, positively-charged particle with many-electron atoms or molecules. This kind of interaction differs qualitatively from the interaction of an electron with an atom or molecule: not only is the sign of charge of the incident light particle different, but the positron wavefunction does not have to be orthogonal to the wavefunctions of the bound electrons, as would be the case for electron–molecule interactions where the Pauli exclusion principle plays a more important role.

One phenomenon that we have studied extensively using stored positrons is the annihilation rates for a range of molecular species. As shown in Fig. 7(a), many molecules have annihilation rates $Z_{\rm eff}$ [as defined in Eq. (4)] that exceed the rates expected on the basis of simple models by as many as six orders of magnitude. For a large class of compounds, namely non-polar molecules having only single bonds, we discovered that $\log Z_{\rm eff}$ is proportional to $(E_i - E_{\rm Ps})^{-1}$ [cf. Fig. 7(b)], where $E_i$ is the ionization energy of the molecule and $E_{\rm Ps} = 6.8$ eV is the binding energy of the positronium atom.[14] We have speculated that this result suggests that the virtual positronium channel plays an important role in the high annihilation rates observed for the hydrocarbons.[25,23] Recent calculations confirm the importance of including these positronium levels in the calculation of molecular annihilation rates for these molecules.[138]

Another aspect of these experiments is the ability to study the Doppler broadening of the 511 keV annihilation line. The broadening of this line is dominated by the momentum of the annihilated electron, and therefore provides information about the electronic environment of the positron annihilation site. In Fig. 8, we show the annihilation line from

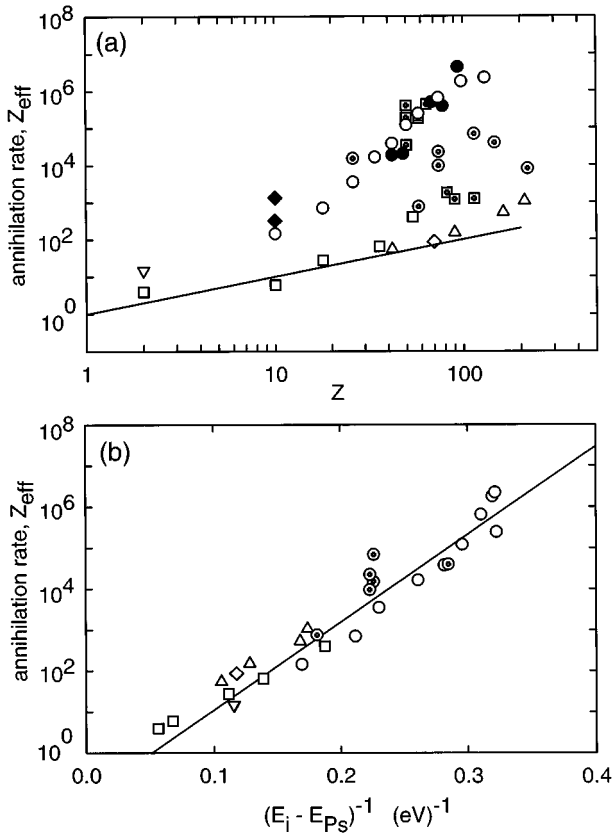


FIG. 7. (a) Positron annihilation rate $Z_{\text{eff}}$ for single-bonded non-polar molecules as a function of $Z$; solid line $Z_{\text{eff}}=Z$; (b) $Z_{\text{eff}}$ as a function of $E_i-E_{\text{Ps}}$, where $E_{\text{Ps}}=6.8$ eV is the binding energy of the positronium atom. Solid line: linear regression.

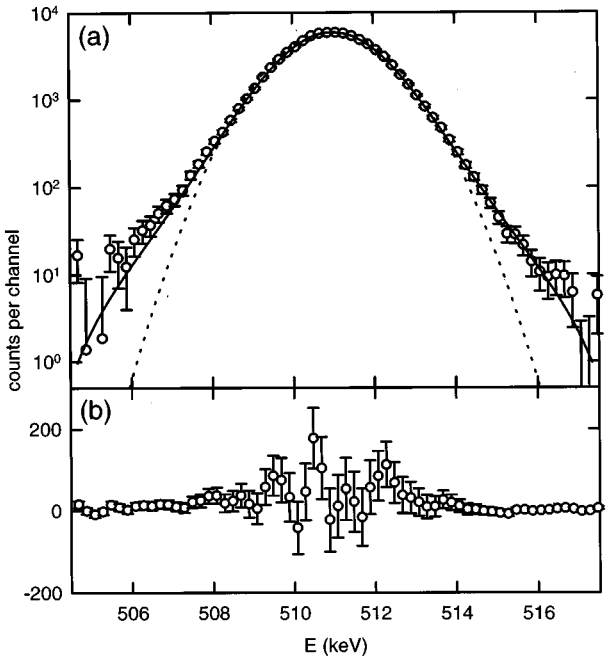


FIG. 8. (a) Annihilation $\gamma$-ray spectrum for positrons annihilating on helium atoms: (○) experimental measurements; solid line: theoretical predictions (Ref. 139); dashed line: Gaussian fit. (b) Residuals from the theoretical calculation.

helium,[139] measured using a high-resolution intrinsic germanium detector. Also shown is the prediction of a new theoretical calculation. This figure demonstrates the good agreement between theory and experiment that can now be obtained, at least for relatively simple atoms such as helium.

### 3. Positron ionization mass spectrometry

When a positron annihilates with an electron in a molecule, it produces a positive ion. These ions have been studied by time-of-flight techniques.[140,141] This process is qualitatively different from ionization by electron impact, and consequently it may provide additional information and enable new techniques for mass spectrometry. An important discovery in this area is that positrons with energies slightly above the positronium formation threshold ($E_i-E_{\text{Ps}}$) can produce unfragmented ions, and this might aid in chemical identification.[142] An example of this effect is illustrated in Fig. 9, which shows the mass spectra from dodecane ($C_{12}H_{26}$): the parent ion dominates the spectrum for positrons with energies of 3.5 eV, which is $\sim$1.5 V above the positronium formation threshold. Related studies have provided additional information about the nature of the interaction of positron with molecules.[143]

### 4. Astrophysical simulations

Positron–atom and positron–molecule interactions are directly relevant to understanding the interaction of galactic positrons with the interstellar medium (ISM). This process produces a strong galactic annihilation $\gamma$-ray line.[145,136] The nature of this phenomenon is a current research topic in $\gamma$-ray astronomy. We have recently shown that positron annihilation on large molecules could, in principle, produce a significant fraction of the annihilation radiation coming from the interstellar medium.[26] This was done by studying the annihilation $\gamma$-radiation from positrons interacting with a simulated interstellar medium consisting of hydrogen with a small admixture of the polycyclic aromatic hydrocarbon, naphthalene.[27]

### 5. Use of positrons to study plasma transport

We have proposed that positrons can be used as test particles to study transport in plasmas.[146,147] Such experiments could contribute to our fundamental understanding of plasma behavior in that they could provide an easily detectable, electron-mass test particle to study plasma transport. From a practical point of view, understanding the turbulent transport of particles and energy is an important issue in the quest to develop a useful source of electrical energy from controlled fusion.

We envisioned that a radioactive source, moderator, and positron accumulator, such as those described in Sec. III, could provide a suitable pulsed source of positrons. Near the edge of the fusion plasma (e.g., confined in a tokamak), the positrons would be converted to neutral positronium atoms by charge-exchange with neutral hydrogen.[148] Positronium atoms entering the plasma would then become ionized, much like the neutral hydrogen beams currently used for plasma heating. The subsequent transport of the positrons (e.g., by

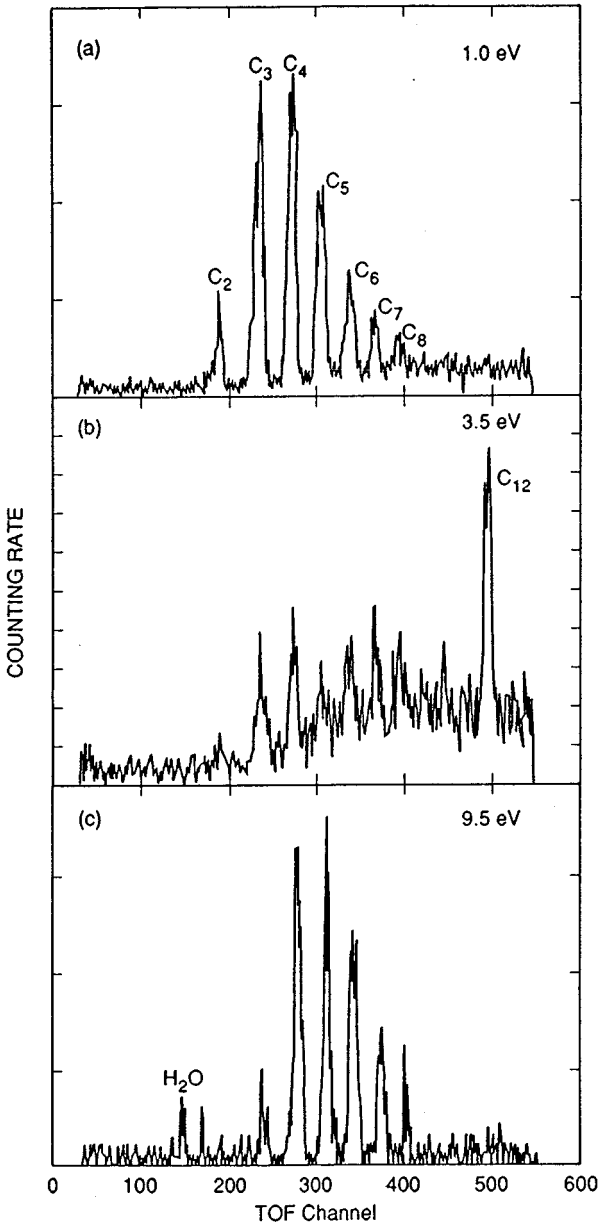


FIG. 9. Mass spectra of ion fragments from dodecane, induced by positrons at three incident energies: (a) below the positronium formation threshold; (b) slightly above the threshold; (c) far above the threshold (from Ref. 144). Electron impact ionization produces extensive fragmentation similar to (c).

convection and diffusion) out of the plasma would be monitored by measuring the time required for them to reach the ''limiter'' or ''divertor plates,'' which typically serve to define the plasma edge. The arrival of the positrons would be measured by a $\gamma$-ray detector located near the limiter.

Such positron transport experiments could help to establish the role which transport along the magnetic field plays (e.g., in contrast to $\mathbf{E}\times\mathbf{B}$ drifts across the magnetic field) in producing the anomalously large transport observed in many tokamak experiments. As described in Sec. III C, we have now exceeded the original design goals for the positron source proposed for this experiment by more than one order of magnitude.

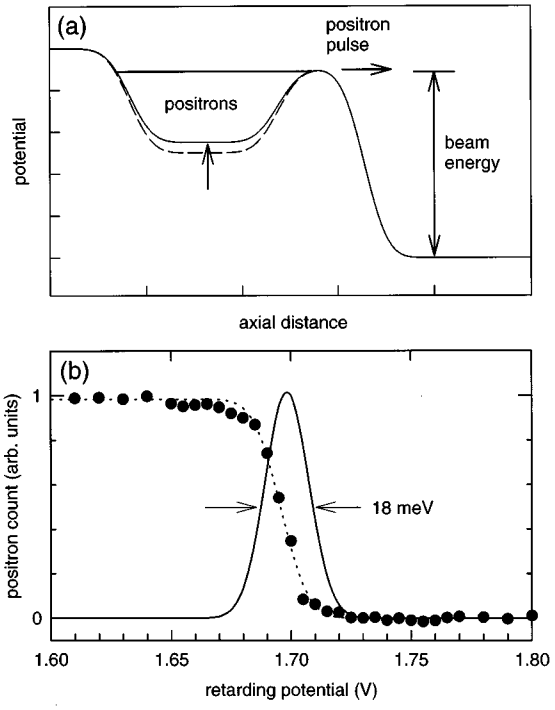


FIG. 10. (a) Electrostatic potential in a positron trap for producing cold pulsed beams of positrons. (b) Energy spread of a typical pulsed beam, measured using a retarding potential energy analyzer; (●) number of positrons reaching the collector as a function of the retarding potential; dotted line: fitted error function; solid line: energy distribution function of the beam, calculated by differentiating the fit to the data.

### 6. Pulsed positron beams

Positron beams have a variety of scientific and technological uses, including atomic physics experiments,[3] characterizing solids and surfaces,[4] and positron microscopy.[149] For many of these applications, high brightness, pulsed beams with very low emittance are required. We have recently developed such a source by releasing cold positrons from a trap in a controlled way.[70] Figure 10(a) shows a schematic diagram for producing both pulsed and quasi-steady state beams. Positrons are accumulated in the trap in the usual way and are then released by raising the potential on the central confining electrode to allow the positrons to ''spill out'' over the gate electrode. By steady ramping of the potential, a quasi-steady state beam is produced, and by applying a staircase potential, a series of pulses can be produced. Figure 10(b) shows an example of the narrow energy spread that can be obtained.

### 7. Antihydrogen production

Both positrons and antiprotons are required for the production of antihydrogen. For this purpose, the positrons are required to be in an UHV (ultrahigh vacuum) environment. The magnetron drift technique can accumulate positrons directly in UHV, but the trapping rates are very low. Modifications to the buffer gas method have recently been proposed that will allow high-efficiency accumulation of positrons in an UHV environment. The resulting positron plasmas are expected to be suitable for the production of antihydrogen.[103] Briefly, this scenario involves pumping the buffer gas out of

the trap after the positrons have been trapped, and then transferring them to a separate UHV stage, which would be isolated from the trap by a gate valve during the time when the buffer gas is admitted.

#### 8. Other experiments

There are a number of areas where large accumulations of positrons and high density positron gases and plasmas could lead to new capabilities. While achieving such conditions is far beyond anything that has been done to date (e.g., densities in excess of $10^{16}\,\mathrm{cm}^{-3}$), there are concrete proposals to reach such regimes.

Platzman and Mills[150] considered the Bose condensation of positronium atoms, predicting that this effect can be isolated and studied in the regime in which the system is a weakly interacting Bose gas. They propose a clever scheme to produce the high density positronium gas necessary for this experiment and for others that require high density electron–positron plasmas. In this scenario, a 5 ns burst of $10^6$ positrons is focused to a 1 $\mu$m spot on the surface of a silicon crystal, using electrostatic optics and remoderation techniques. Just below the surface, a cylindrical void 1000 Å in diameter by 1 $\mu$m long is etched in the crystal, with the axis of the cylinder orientated parallel to the surface. They estimate that a $10^{18}\,\mathrm{cm}^{-3}$ density collection of triplet positronium atoms will be left following the rapid 2-$\gamma$ decay of the singlet atoms. Subsequent cooling of the positronium by the crystal is expected to bring the system into the Bose condensed state. The signature of Bose condensation is expected to appear as a zero-momentum peak in the momentum distribution of the positronium atoms, and it could be measured by the standard ACAR (angular correlation of annihilation radiation) technique following the quenching of the metastable triplet atoms by a magnetic field.

The possibility of making an annihilation $\gamma$-ray laser at 511 keV has also been discussed.[151,152] Unfortunately, gain (i.e., significant stimulated emission) at 511 keV is predicted to require densities of positrons virtually unimaginable in the laboratory. The annihilation line will be broadened due to the fact that both the positrons and electrons will be degenerate Fermi gases.[152] As a consequence, the required density is of the order of $10^{32}\,\mathrm{cm}^{-3}$, and so lasing action at this wavelength is likely to occur only in dense, compact astrophysical objects such as pulsars.

A third experiment utilizing a high density positron plasmas is the study of possible resonances in the interaction of electrons and positrons at energies of the order of 1 MeV. In order to avoid complications arising from atomic and nuclear effects, it has been proposed to investigate this effect using a MeV energy electron beam impinging on a high density positron plasma.[153] In this case, the plasma would be created by intense bursts of positrons generated by a LINAC and confined in vacuum in a standard Malmberg–Penning trap.

Finally, the possibility of using positron plasmas to cool highly charged ions for precision spectroscopy has also been discussed.[154]

### B. Uses of antiprotons

The confinement of antiprotons in traps opens up many new areas for study including atomic physics, antimatter gravity studies, and the possibility of antihydrogen production. Antiprotons are currently available only at a few high-energy facilities. Thus the availability of portable Penning traps could permit the transportation of trapped antiprotons to laboratories around the world for a variety of scientific and technological applications. Traps of this type are now under development.[155] In a first demonstration experiment, an electron plasma has been transported across the continental United States.[156]

#### 1. Pulsed beams

Cold beams of pulsed antiprotons are desirable for a range of atomic physics experiments such as measurements of collision cross-sections[157] and the production and study of exotic atoms.[158] Such beams could be produced in the same way as the pulsed positron beams described in Sec. VI A 6. Using this technique, the beam energy could be varied over a wide range from less than 1 eV to tens of kilovolts.

#### 2. Exotic atoms

Antiprotons can form compound molecules with ordinary matter, and some of these molecules exist in long-lived metastable states.[158] Following their discovery, metastable antiprotonic atoms such as $\overline{p}\mathrm{He}^{+}$ have attracted a great deal of attention, both theoretically and experimentally.[159–161] A recent highlight of experiments in this area has been the observation of laser-induced resonant annihilation,[162] illustrated in Fig. 11. Experiments to date have been confined to condensed media and dense gases which are not ideal for precision measurements. Using antiprotons from a Penning trap, it is expected that atomic beams of these and other exotic antiprotonic atoms such as $\overline{p}\mathrm{He}^{++}$ and protonium (i.e., $\overline{pp}$) could be created, thus leading to new scientific opportunities.

#### 3. Gravity

Direct measurement of the gravitational mass of the positron is very difficult because of the stringent requirement on shielding stray electric fields.[163] (An earlier experiment that reported a measurement of the gravitational mass of the electron has been the subject of some controversy.[164]) It has been pointed out that such measurements might be conducted more easily using antiprotons, because of the much lower charge-to-mass ratio.[165] Various techniques for measuring the gravitational mass of the antiproton have been discussed.[166] One method involves launching antiprotons vertically from a Penning trap into a field-free drift tube and measuring the time of flight.[167] Another method proposes measuring the gravitational shift in the center of mass of antiprotons in a Penning trap.[168]

#### 4. Medical uses

Several medical uses for antiprotons have been discussed in the literature[155] including radiopharmaceutical production for positron emission tomography (PET), and medical imaging and radiotherapy. For PET, the short-lived

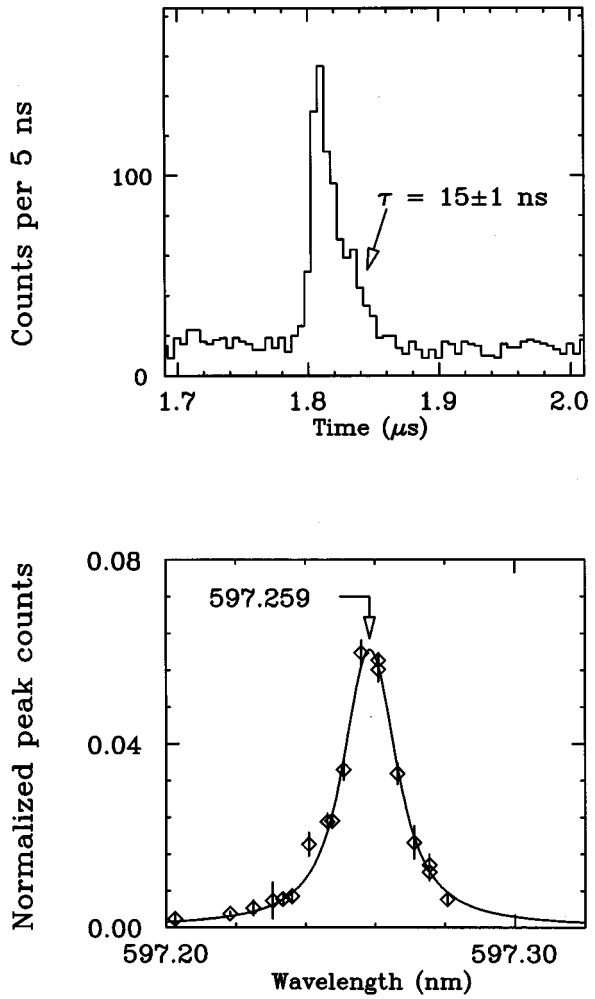


FIG. 11. Above: Time dependence of the delayed annihilation of antiprotons in $\bar{p}\mathrm{He}^{+}$ induced by laser irradiation at 597.259 nm, and below: lineshape of the resonance (after Ref. 162).

isotope $^{15}$O can be produced by reactions of $^{16}$O with antiprotons and antiproton annihilation fragments. By the use of antiprotons transported to end users in portable traps, the expense of an on-site cyclotron could be avoided, and PET could be made more widely available. Estimates in Ref. 155 suggest that, in comparison with existing techniques, such a system might be made cost-effective with envisaged improvements to existing technology.

Proton radiotherapy is a rapidly advancing field because the reasonably narrow stopping distance of high-energy protons allows precise targeting of tumors. It has been pointed out that antiprotons offer some advantages over protons in that their stopping distance is even narrower, and furthermore, the penetrating annihilation pions can be imaged externally.[155] Thus the annihilation vertex can be precisely reconstructed, permitting real-time monitoring of treatment.

#### 5. Antihydrogen

As discussed in Sec. V, an important use for cold antiprotons in Penning traps is the production of antihydrogen. Accumulations of antiprotons reported to date are sufficiently cold and dense for this purpose.

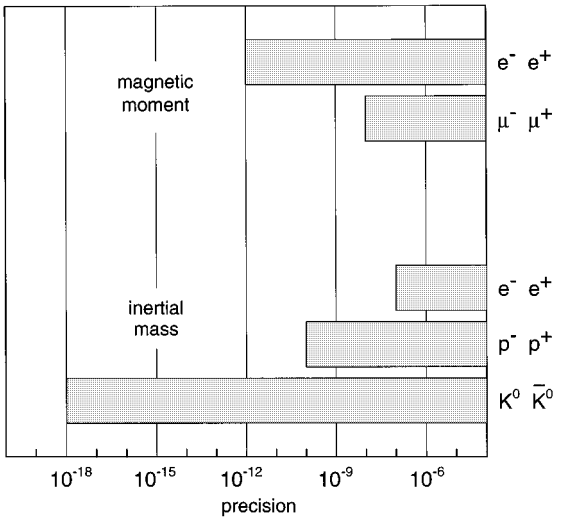


FIG. 12. Summary of the present status of measurements of fundamental tests of the CPT theorem comparing properties of particles and antiparticles.

### C. Uses of antihydrogen

#### 1. Spectroscopy

One fundamental interest in creating antihydrogen arises from the possibility of making stringent tests of the CPT theorem.[32] One important implication of this theorem is that particles and their antiparticles have the same inertial masses and lifetimes. Some of these predictions have been tested to very high precision. In the weak sector, a test of the equality of the $K^0$ and $\overline{K^0}$ masses[169] has set the scale of precision at $10^{-18}$. However, this CPT test is based on an indirect and model-dependent connection between the measured properties of the decay amplitudes and the kaon mass matrix. For electromagnetic interactions, the implication of the CPT theorem is that particles and their antiparticles have masses that are equal, and charges and gyromagnetic moments that are equal in magnitude but opposite in sign. Direct tests in the electromagnetic sector have achieved good precision. Examples include the equality of the electron and positron gyromagnetic ratios (accurate to $2.1\times10^{-12}$)[9] and the equality of the proton and antiproton cyclotron frequencies in the same magnetic field (accurate to $10^{-9}$).[20] The present status of CPT tests is summarized in Fig. 12.

The availability of trapped antihydrogen would permit many other tests of the predictions of CPT for quantum electrodynamics, such as the equivalence of the fine structure, the hyperfine structure, and the Lamb shift. They could also provide tests of CPT at a level comparable to that achieved in the $K^0\overline{K^0}$ system. Spectroscopic measurements of photon transition frequencies in antihydrogen could, in principle, be performed with very high precision, and consequently comparison with the analogous transitions in hydrogen would test CPT invariance with commensurate precision. In particular, the 1/8-second lifetime of the metastable $2S$ level would allow an ultimate precision of the $1S-2S$ two-photon transition of $10^{-18}$, if the center of the spectral line can be determined to one part in $10^3$ and the line width can be reduced to the quantum limit.[170] For a more detailed discussion of these and related issues see Ref. 32.

### 2. Gravity

A second topic of interest using antihydrogen concerns study of the gravitational attraction of matter and antimatter. The proof of CPT invariance requires the assumption of flat spacetime.[171] There is no CPT theorem in the curved spacetime required by general relativity. This places a limit on our understanding of the relationship of particle physics and gravitation. A number of attempts to unify gravity with the electro-weak and strong interactions have been made. Many of them call into question the general belief that the gravitational acceleration of particles and their antiparticles should be identical.[166] However, no direct experimental tests have been performed.

Spectroscopic methods applied to atomic fountains have been used to determine the gravitational acceleration of atoms with an accuracy of $10^{-8}$ and such methods could also be applied to antihydrogen.[172] Other possible gravitational measurements using antihydrogen include ballistic methods[173] and atom interferometry.[174]

## VII. CONCLUDING REMARKS

In this paper we have reviewed recent progress in low-energy antimatter research. Plasma physics techniques have been and will continue to be central to these efforts. Large numbers of positrons ($\sim 10^8$) and antiprotons ($\sim 10^6$) can now be accumulated in Penning traps. These collections of antimatter have already been employed to study a number of physics issues. These advances in the trapping of positrons and antiprotons have made the production and trapping of antihydrogen a real possibility. Furthermore, the potential availability of portable traps for the transportation of antiprotons offers a wide variety of new scientific and technological possibilities. New capabilities such as those discussed in this paper will continue to be driven by the development of techniques to create and manipulate antimatter plasmas.

## ACKNOWLEDGMENTS

We wish to acknowledge helpful conversations with M. Charlton, S. Gilbert, M. Holzscheiter, K. Iwata, C. Kurz, A. P. Mills, Jr., and G. A. Smith.

The work at UCSD is supported by the Office of Naval Research under Grant No. N00014-96-10579 and the National Science Foundation under Grant No. PHY 9600407.

[1]C. D. Anderson, Science **76**, 238 (1932).
[2]L. E. Feinendegen, H. Herzog, and T. Kuwert, Mat. Sci. Forum **105–110**, 51 (1992).
[3]A. P. Mills, Jr., Science **218**, 335 (1982).
[4]P. J. Schultz and K. G. Lynn, Rev. Mod. Phys. **60**, 701 (1988).
[5]G. Gibson, W. C. Jordan, and E. J. Lauer, Phys. Rev. Lett. **5**, 141 (1960).
[6]H. Dehmelt, Rev. Mod. Phys. **62**, 525 (1990).
[7]H. G. Dehmelt, P. B. Schwinberg, and R. S. Van Dyck, Jr., Int. J. Mass Spectrom. Ion Phys. **26**, 107 (1978).
[8]P. B. Schwinberg, R. S. Van Dyck, Jr., and H. G. Dehmelt, Phys. Lett. A **81**, 119 (1981).
[9]R. S. Van Dyck, Jr., P. B. Schwinberg, and H. G. Dehmelt, Phys. Rev. Lett. **59**, 26 (1987).
[10]J. H. Malmberg and J. S. de Grassie, Phys. Rev. Lett. **35**, 577 (1975).
[11]J. H. Malmberg and C. F. Driscoll, Phys. Rev. Lett. **44**, 654 (1980).
[12]T. M. O'Neil, Comments Plasma Phys. Controlled Fusion **5**, 213 (1980).
[13]C. M. Surko, M. Leventhal, and A. Passner, Phys. Rev. Lett. **62**, 901 (1989).
[14]T. J. Murphy and C. M. Surko, Phys. Rev. A **46**, 5696 (1992).
[15]R. G. Greaves, M. D. Tinkle, and C. M. Surko, in *Nonneutral Plasma Physics II*, edited by J. Fajans and D. H. E. Dubin (American Institute of Physics, New York, 1995), pp. 70–86.
[16]G. Gabrielse, X. Fei, K. Helmerson, S. L. Rolston, R. Tjoelker, T. A. Trainor, H. Kalinowsky, J. Haas, and W. Kells, Phys. Rev. Lett. **57**, 2504 (1986).
[17]G. Gabrielse, X. Fei, L. A. Orozco, R. L. Tjoelker, J. Haas, H. Kalinowsky, T. A. Trainor, and W. Kells, Phys. Rev. Lett. **63**, 1360 (1989).
[18]M. H. Holzscheiter, Hyperfine Interact. **81**, 71 (1993).
[19]M. H. Holzscheiter, X. Feng, T. Goldman, N. S. P. King, R. A. Lewis, M. M. Nieto, and G. A. Smith, Phys. Lett. A **214**, 279 (1996).
[20]G. Gabrielse, D. Phillips, W. Quint, H. Kalinowsky, G. Rouleau, and W. Jhe, Phys. Rev. Lett. **74**, 3544 (1995).
[21]T. J. Murphy and C. M. Surko, Phys. Rev. Lett. **67**, 2954 (1991).
[22]S. Tang, M. D. Tinkle, R. G. Greaves, and C. M. Surko, Phys. Rev. Lett. **68**, 3793 (1992).
[23]K. Iwata, R. G. Greaves, T. J. Murphy, M. D. Tinkle, and C. M. Surko, Phys. Rev. A **51**, 473 (1995).
[24]C. Kurz, R. G. Greaves, and C. M. Surko, Phys. Rev. Lett. **77**, 2929 (1996).
[25]C. M. Surko, A. Passner, M. Leventhal, and F. J. Wysocki, Phys. Rev. Lett. **61**, 1831 (1988).
[26]C. M. Surko, R. G. Greaves, and M. Leventhal, Hyperfine Interact. **81**, 239 (1993).
[27]K. Iwata, R. G. Greaves, and C. M. Surko, Can. J. Phys. **51**, 407 (1996).
[28]B. L. Brown, M. Leventhal, and A. P. Mills, Jr., Phys. Rev. A **33**, 2281 (1986).
[29]R. G. Greaves, M. D. Tinkle, and C. M. Surko, Phys. Plasmas **1**, 1439 (1994).
[30]R. G. Greaves and C. M. Surko, Phys. Rev. Lett. **75**, 3846 (1995).
[31]G. Baur, G. Boero, S. Brauksiepe, A. Buzzo, W. Eyrich, R. Geyer, D. Grzonka, J. Hauffe, K. Kilian, M. LoVetere, M. Macri, M. Moosburger, R. Nellen, W. Oelert, S. Passaggio, A. Pozzo, K. Roehrich, K. Sachs, G. Schepers, T. Sefzick, R. S. Simon, R. Stratmann, F. Stinzing, and M. Wolke, Phys. Lett. B **368**, 251 (1996).
[32]M. Charlton, J. Eades, D. Horvath, R. J. Hughes, and C. Zimmermann, Phys. Rep. **241**, 65 (1994).
[33]M. Murakami and L. M. Lidsky, Phys. Rev. Lett. **24**, 297 (1970).
[34]J. S. deGrassie and J. H. Malmberg, Phys. Fluids **23**, 63 (1980).
[35]C. F. Driscoll, K. S. Fine, and J. H. Malmberg, Phys. Fluids **29**, 2015 (1986).
[36]B. R. Beck, J. Fajans, and J. H. Malmberg, Phys. Rev. Lett. **68**, 317 (1992).
[37]B. R. Beck, J. Fajans, and J. H. Malmberg, Phys. Plasmas **3**, 1250 (1996).
[38]C. F. Driscoll and J. H. Malmberg, Phys. Rev. Lett. **50**, 167 (1983).
[39]C. F. Driscoll, J. H. Malmberg, and K. S. Fine, Phys. Rev. Lett. **60**, 1290 (1988).
[40]R. W. Gould, Phys. Plasmas **2**, 2151 (1995).
[41]J. Notte, A. J. Peurrung, J. Fajans, R. Chu, and J. S. Wurtele, Phys. Rev. Lett. **69**, 3056 (1992).
[42]A. J. Peurrung and J. Fajans, Phys. Fluids A **5**, 493 (1993).
[43]D. L. Eggleston and J. H. Malmberg, Phys. Rev. Lett. **59**, 1675 (1987).
[44]J. J. Bollinger, D. J. Wineland, and D. H. E. Dubin, Phys. Plasmas **1**, 1403 (1994).
[45]G. Gabrielse, L. Haarsma, and S. L. Rolston, Int. J. Mass Spectrom. Ion Processes **88**, 319 (1989).
[46]C. F. Driscoll, in *Low Energy Antimatter*, edited by D. B. Cline (World Scientific, Singapore, 1986), pp. 184–95.
[47]T. B. Mitchell, M. H. Holzscheiter, M. M. Schauer, D. W. Scudder, and D. C. Barnes, AIP Conf. Proc. **331**, 113 (1995).
[48]R. G. Greaves, M. D. Tinkle, and C. M. Surko, Phys. Rev. Lett. **74**, 90 (1995).
[49]M. D. Tinkle, R. G. Greaves, and C. M. Surko, Phys. Plasmas **3**, 749 (1996).
[50]L. Brillouin, Phys. Rev. **67**, 260 (1945).
[51]T. M. O'Neil, Phys. Fluids **23**, 2216 (1980).
[52]C. S. Weimer, J. J. Bollinger, F. L. Moore, and D. J. Wineland, Phys. Rev. A **49**, 3842 (1994).
[53]R. C. Davidson, N. A. Krall, K. Papadopoulos, and R. Shanny, Phys. Rev. Lett. **24**, 579 (1970).
[54]S. A. Prasad and T. M. O'Neil, Phys. Fluids **22**, 278 (1979).

[55]J. J. Bollinger, D. J. Heinzen, F. L. Moore, W. M. Itano, D. J. Wineland, and D. H. E. Dubin, Phys. Rev. A **48**, 525 (1993).
[56]T. M. O'Neil and P. G. Hjorth, Phys. Fluids **28**, 3241 (1985).
[57]M. E. Glinsky, T. M. O'Neil, M. N. Rosenbluth, K. Tsuruta, and S. Ichimaru, Phys. Fluids B **4**, 1156 (1992).
[58]C. F. Driscoll and K. S. Fine, Phys. Fluids B **2**, 1359 (1990).
[59]K. S. Fine, A. C. Cass, W. G. Flynn, and C. F. Driscoll, Phys. Rev. Lett. **75**, 3277 (1995).
[60]T. M. O'Neil, Phys. Rev. Lett. **55**, 943 (1985).
[61]D. H. E. Dubin and T. M. O'Neil, Phys. Rev. Lett. **60**, 1286 (1988).
[62]C. L. Longmire and M. N. Rosenbluth, Phys. Rev. **103**, 507 (1956).
[63]A. Simon, Phys. Rev. **100**, 1557 (1955).
[64]F. Anderegg, X.-P. Huang, C. F. Driscoll, E. M. Hollmann, T. M. O'Neil, and D. H. E. Dubin, Phys. Rev. Lett. **78**, 2128 (1997).
[65]T. M. O'Neil, Phys. Fluids **23**, 725 (1980).
[66]D. J. Wineland, C. S. Weimer, and J. J. Bollinger, Hyperfine Interact. **76**, 115 (1993).
[67]D. A. Church and H. G. Dehmelt, J. Appl. Phys. **40**, 3421 (1969).
[68]D. J. Heinzen, J. J. Bollinger, F. L. Moore, W. M. Itano, and D. J. Wineland, Phys. Rev. Lett. **66**, 2080 (1991).
[69]X.-P. Huang, F. Anderegg, E. M. Hollmann, C. F. Hollmann, and T. M. O'Neil, Phys. Rev. Lett. **78**, 875 (1997).
[70]S. J. Gilbert, C. Kurz, R. G. Greaves, and C. M. Surko, ''Creation of a monoenergetic pulsed positron beam,'' J. Appl. Phys. (in press).
[71]L. S. Brown and G. Gabrielse, Rev. Mod. Phys. **58**, 233 (1986).
[72]L. Bracci, G. Fiorentini, and O. Pitzurra, Phys. Lett. B **85**, 280 (1979).
[73]D. Boyd, W. Carr, R. Jones, and M. Seidl, Phys. Lett. A **45**, 421 (1973).
[74]D. L. Eggleston, C. F. Driscoll, B. R. Beck, A. W. Hyatt, and J. H. Malmberg, Phys. Fluids B **4**, 3432 (1992).
[75]M. D. Tinkle, R. G. Greaves, C. M. Surko, R. L. Spencer, and G. W. Mason, Phys. Rev. Lett. **72**, 352 (1994).
[76]M. D. Tinkle, R. G. Greaves, and C. M. Surko, Phys. Plasmas **2**, 2880 (1995).
[77]D. H. E. Dubin, Phys. Rev. Lett. **66**, 2076 (1991).
[78]R. L. Spencer, AIP Conf. Proc. **331**, 204 (1995).
[79]G. W. Mason, R. L. Spencer, and J. A. Bennett, Phys. Plasmas **3**, 1502 (1996).
[80]R. H. Howell, I. J. Rosenberg, and M. J. Fluss, Appl. Phys. A **43**, 247 (1987).
[81]A. Mohri, T. Mischishita, T. Yuyama, and H. Tanaka, Jpn. J. Appl. Phys. Part 2 **30**, L936 (1991).
[82]B. Krusche and K. Schreckenbach, Nucl. Instrum. Methods Phys. Res. A **295**, 155 (1990).
[83]K. G. Lynn and F. M. Jacobsen, Hyperfine Interact. **89**, 19 (1994).
[84]C. Gonzalez-Lepera, Nucl. Instrum. Methods Phys. Res. B **99**, 824 (1995).
[85]M. Hirose, M. Washio, and K. Takahashi, Appl. Surf. Sci. **85**, 111 (1995).
[86]M. Charlton and G. Laricchia, Hyperfine Interact. **76**, 97 (1993).
[87]E. Gramsch, J. Throwe, and K. G. Lynn, Appl. Phys. Lett. **51**, 1862 (1987).
[88]N. Zafar, J. Chevallier, G. Laricchia, and M. Charlton, J. Phys. D **22**, 868 (1989).
[89]A. P. Mills, Appl. Phys. Lett. **37**, 667 (1980).
[90]B. L. Brown, W. S. Crane, and A. P. Mills, Jr., Appl. Phys. Lett. **48**, 739 (1986).
[91]A. P. Mills, Jr. and E. M. Gullikson, Appl. Phys. Lett. **49**, 1121 (1986).
[92]R. Khatri, M. Charlton, P. Sferlazzo, K. G. Lynn, A. P. Mills, Jr., and L. O. Roellig, Appl. Phys. Lett. **57**, 2374 (1990).
[93]G. R. Massoumi, N. Hozhabri, W. N. Lennard, P. J. Schultz, S. F. Baert, H. H. Jorch, and A. H. Weiss, Rev. Sci. Instrum. **62**, 1460 (1991).
[94]R. G. Greaves and C. M. Surko, Can. J. Phys. **51**, 445 (1996).
[95]R. S. Conti, B. Ghaffari, and T. D. Steiger, Hyperfine Interact. **76**, 127 (1993).
[96]B. Ghaffari and R. S. Conti, Phys. Rev. Lett. **75**, 3118 (1995).
[97]T. E. Cowan, B. R. Beck, J. H. Hartley, R. H. Howell, R. R. Rohatgi, J. Fajans, and R. Gopalan, Hyperfine Interact. **76**, 135 (1993).
[98]A. Mohri, H. Tanaka, T. Michishita, Y. Yuyama, Y. Kawase, and T. Takami, in *Elementary Processes in Dense Plasmas*, edited by S. Ichimaru and S. Ogata (Addison–Wesley, New York, 1995), pp. 477–486.
[99]D. L. Donohue, L. D. Hulett, Jr., S. A. McLuckey, G. L. Glish, and H. S. McKown, Int. J. Mass Spectrom. Ion Processes **97**, 227 (1990).
[100]D. Segers, J. Paridaens, M. Dorikens, and L. Dorikens-Vanpraet, Nucl. Instrum. Methods Phys. Res. A **337**, 246 (1994).
[101]F. Ebel, W. Faust, H. Schneider, and I. Tobehn, Nucl. Instrum. Methods Phys. Res. A **274**, 1 (1989).
[102]L. Haarsma, K. Abdullah, and G. Gabrielse, Phys. Rev. Lett. **75**, 806 (1995).
[103]C. M. Surko, R. G. Greaves, and M. Charlton, ''Stored positrons for antihydrogen production,'' Hyperfine Interact. (in press).
[104]S. Baird, J. Bosser, M. Chanel, P. Lefevre, R. Ley, D. Manglunki, S. Maury, D. Mohl, and G. Tranquille, Hyperfine Interact. **76**, 61 (1993).
[105]X. Feng, M. H. Holzscheiter, M. Charlton, F. Cverna, T. Ichioka, N. S. P. King, R. A. Lewis, L. Morgan, J. Rochet, and Y. Yamazaki, Phys. Atom. Nucl. **59**, 1551 (1996).
[106]A. Wolf, Hyperfine Interact. **76**, 189 (1993).
[107]M. E. Glinsky and T. M. O'Neil, Phys. Fluids B **3**, 1279 (1991).
[108]B. I. Deutch, M. Charlton, M. H. Holzscheiter, P. Hvelplund, L. V. Jorgensen, H. Knudsen, G. Laricchia, J. Merrison, and M. Poulsen, Hyperfine Interact. **76**, 153 (1993).
[109]M. Charlton, Phys. Lett. A **143**, 143 (1990).
[110]J. P. Merrison, H. Bluhme, J. Chevallier, B. I. Deutch, P. Hvelplund, L. V. Joergensen, H. Knudsen, M. R. Poulsen, and M. Charlton, ''Hydrogen formation by proton impact on positronium,'' Phys. Rev. Lett. (in press).
[111]W. Quint, R. Kaiser, D. Hall, and G. Gabrielse, Hyperfine Interact. **76**, 181 (1993).
[112]D. S. Hall and G. Gabrielse, Phys. Rev. Lett. **77**, 1962 (1996).
[113]M. Charlton, Can. J. Phys. **74**, 483 (1996).
[114]G. Z. Li, R. Poggiani, G. Testera, G. Torelli, and G. Werth, Hyperfine Interact. **76**, 343 (1993).
[115]J. Walz, C. Zimmermann, L. Ricci, M. Prevedelli, and T. W. Hansch, Phys. Rev. Lett. **75**, 3257 (1995).
[116]J. T. M. Walraven, Hyperfine Interact. **76**, 205 (1993).
[117]C. L. Cesar, D. G. Fried, T. C. Killian, A. D. Polcyn, J. C. Sandberg, I. A. Yu, T. J. Greytak, D. Kleppner, and J. M. Doyle, Phys. Rev. Lett. **77**, 255 (1996).
[118]I. D. Setija, H. G. C. Werij, O. J. Luiten, M. W. Reynolds, T. W. Hijmans, and J. T. M. Walraven, Phys. Rev. Lett. **70**, 2257 (1993).
[119]U. A. Mofiz, Astrophys. Space Sci. **196**, 101 (1992).
[120]G. Henri, G. Pelletier, and J. Roland, Astrophys. J. Lett. **404**, L41 (1993).
[121]T. Kitanishi, J. Sakai, K. Nishikawa, and J. Zhao, Phys. Rev. E **53**, 6376 (1996).
[122]A. D. Rogava, S. M. Mahajan, and V. I. Berezhiani, Phys. Plasmas **3**, 3545 (1996).
[123]J. Zhao, J. I. Sakai, and K. I. Nishikawa, Phys. Plasmas **3**, 844 (1996).
[124]V. I. Berezhiani and S. M. Mahajan, Phys. Rev. Lett. **73**, 1110 (1994).
[125]M. Gedalin, Phys. Rev. Lett. **76**, 3340 (1996).
[126]L. N. Tsintsadze and P. K. Shukla, Phys. Rev. A **46**, 5288 (1992).
[127]G. P. Zank and R. G. Greaves, Phys. Rev. E **51**, 6079 (1995).
[128]N. Iwamoto, Phys. Rev. E **47**, 604 (1993).
[129]G. A. Stewart and E. W. Laing, J. Plasma Phys. **47**, 295 (1992).
[130]V. Tsytovich and C. B. Wharton, Comments Plasma Phys. Controlled Fusion **4**, 91 (1978).
[131]S. Y. Abdul-Rassak and E. W. Laing, J. Plasma Phys. **52**, 309 (1994).
[132]T. M. O'Neil (personal communication, 1996).
[133]H. Boehmer, M. Adams, and N. Rynn, Phys. Plasmas **2**, 4369 (1995).
[134]R. J. Gould, Astrophys. J. **344**, 232 (1989).
[135]N. Guessoum, R. Ramaty, and R. E. Lingenfelter, Astrophys. J. **378**, 170 (1991).
[136]R. Ramaty, J. Skibo, and R. E. Lingenfelter, Astrophys. J., Suppl. Ser., **92**, 393 (1994).
[137]K. Iwata, R. G. Greaves, and C. M. Surko, ''Gamma-ray annihilation spectra from positron–molecule interactions,'' to appear in Phys. Rev. A.
[138]E. P. da Silva, J. S. E. Germane, and M. A. P. Lima, Phys. Rev. Lett. **77**, 1028 (1996).
[139]P. Van Reeth, J. W. Humberston, K. Iwata, R. G. Greaves, and C. M. Surko, J. Phys. B **29**, L465 (1996).
[140]A. Passner, C. M. Surko, M. Leventhal, and A. P. Mills, Jr., Phys. Rev. A **39**, 3706 (1989).
[141]G. L. Glish, R. G. Greaves, S. A. McLuckey, L. D. Hulett, C. M. Surko, J. Xu, and D. L. Donohue, Phys. Rev. A **49**, 2389 (1994).
[142]L. D. Hulett, Jr., D. L. Donohue, J. Xu, T. A. Lewis, S. A. McLuckey, and G. L. Glish, Chem. Phys. Lett. **216**, 236 (1993).
[143]J. Xu, L. D. Hulett, Jr., T. A. Lewis, and S. A. McLuckey, Phys. Rev. A **52**, 2088 (1995).
[144]L. D. Hulett, Jr., J. Xu, S. McLuckey, T. Lewis, and D. Schrader, Can. J. Phys. **74**, 411 (1996).
[145]R. W. Bussard, R. Ramaty, and R. J. Drachman, Astrophys. J. **228**, 928 (1979).

[146]C. M. Surko, M. Leventhal, W. S. Crane, A. Passner, and F. Wysocki, Rev. Sci. Instrum. **57**, 1862 (1986).
[147]T. J. Murphy, Plasma Phys. Controlled Fusion **29**, 549 (1987).
[148]S. Tang and C. M. Surko, Phys. Rev. A **47**, 743 (1993).
[149]L. D. Hulett, Jr., Mat. Sci. Forum **175–178**, 99 (1995).
[150]P. M. Platzman and J. P. Mills, Jr., Phys. Rev. B **49**, 454 (1994).
[151]M. Bertolotti and C. Sibilia, Appl. Phys. **19**, 127 (1979).
[152]C. M. Varma, Nature **267**, 686 (1977).
[153]T. E. Cowan, J. Hartley, R. H. Howell, J. L. McDonald, R. R. Rohatgi, and J. Fajans, Mat. Sci. Forum **105–110**, 529 (1992).
[154]D. A. Church, Phys. Scr. **46**, 278 (1992).
[155]R. A. Lewis, G. A. Smith, and S. D. Howe, ''Antiproton portable traps and medical applications,'' to appear in Hyperfine Interact.
[156]C. H. Tseng and G. Gabrielse, Hyperfine Interact. **76**, 381 (1993).
[157]H. Knudsen, U. Mikkelsen, K. Paludan, K. Kirsebom, S. P. Moller, E. Uggerhoj, J. Slevin, M. Charlton, and E. Morenzoni, J. Phys. B **28**, 3569 (1995).
[158]G. Backenstoss, Contemp. Phys. **30**, 433 (1989).
[159]J. D. Davies, T. P. Gorringe, J. Lowe, J. M. Nelson, S. M. Playfer, G. J. Pyle, G. T. A. Squier, C. A. Baker, C. J. Batty, S. A. Clark, S. Sakamoto, R. E. Welsh, R. G. Winter, and E. W. A. Lingeman, Phys. Lett. B **145**, 319 (1984).
[160]T. Yamazaki, E. Widmann, R. S. Hayano, M. Iwasaki, S. N. Nakamura, K. Shigaki, F. J. Hartmann, H. Daniel, T. von Egidy, P. Hofmann, Y.-S. Kim, and J. Eades, Nature **361**, 238 (1993).
[161]P. T. Greenland and R. Thurwachter, Hyperfine Interact. **76**, 355 (1993).
[162]N. Morita, M. Kumakura, T. Yamazaki, E. Widmann, H. Masuda, I. Sugai, R. S. Hayano, F. E. Maas, H. A. Torii, F. J. Hartmann, H. Daniel, T. von Egidy, B. Ketzer, W. Muller, W. Schmid, D. Horvath, and J. Eades, Phys. Rev. Lett. **72**, 1180 (1994).
[163]T. W. Darling, F. Rossi, G. I. Opat, and G. F. Moorhead, Rev. Mod. Phys. **64**, 237 (1992).
[164]F. C. Witteborn and W. M. Fairbank, Phys. Rev. Lett. **19**, 1049 (1967).
[165]T. Goldman and M. M. Nieto, Phys. Lett. B **112**, 437 (1982).
[166]M. M. Nieto and T. Goldman, Phys. Rep. **205**, 221 (1991).
[167]P. Dyer, J. Camp, M. H. Holzscheiter, and S. Graessle, Nucl. Instrum. Methods Phys. Res. B **40–41**, 485 (1988).
[168]V. Lagomarsino, V. Lia, G. Manuzio, and G. Testera, Phys. Rev. A **50**, 977 (1994).
[169]R. Carosi, P. Clarke, D. Coward, D. Cundy, N. Doble, L. Gatignon, V. Gibson, P. Grafstrom, R. Hagelberg, G. Kesseler, J. van der Lans, H. N. Nelson, H. Wahl, R. Black, D. J. Candlin, J. Muir, K. J. Peach, H. Blumer, R. Heinz, M. Kasemann, K. Kleinknecht, P. Mayer, B. Panzer, V. Renk, S. Roehn, H. Rohrer, E. Auge, R. L. Chase, D. Fournier, P. Heusse, L. Iconomidou-Fayard, I. Harrus, A. M. Lutz, A. C. Schaffer, L. Bertanza, A. Bigi, P. Calafiura, M. Calvetti, R. Casali, C. Cerri, R. Fantechi, G. Gargani, I. Mannelli, A. Nappi, G. M. Pierazzini, C. Becker, H. Burkhardt, M. Holder, G. Quast, M. Rost, H. G. Sander, W. Weihs, and G. Zech, Phys. Lett. B **237**, 303 (1990).
[170]D. H. McIntyre and T. W. Hänsch, Metrologia **25**, 61 (1988).
[171]R. M. Wald, Phys. Rev. D **21**, 2742 (1980).
[172]M. Kasevich and S. Chu, Appl. Phys. B **54**, 321 (1992).
[173]N. Beverini, V. Lagomarsino, G. Manuzio, R. Poggiani, F. Scuri, and G. Torelli, Phys. Lett. B **206**, 533 (1988).
[174]T. J. Phillips, in *Proceedings of the 3rd Biennial Conference on Low Energy Antiproton Physics*, edited by G. Kernel, P. Krizan, and M. Mikuz (World Scientific, Singapore, 1995), pp. 569–578.